

Effect of Dynamical Coulomb Correlations on the Fermi Surface of $\text{Na}_{0.3}\text{CoO}_2$

H. Ishida¹, M.D. Johannes², and A. Liebsch³

¹College of Humanities and Sciences, Nihon University, Sakura-josui, Tokyo 156, Japan

²Code 6391, Naval Research Laboratory, Washington, D.C. 20375, USA

³Institut für Festkörperforschung, Forschungszentrum Jülich, 52425 Jülich, Germany

The t_{2g} quasi-particle spectra of $\text{Na}_{0.3}\text{CoO}_2$ are calculated within the dynamical mean field theory. It is shown that as a result of dynamical Coulomb correlations charge is transferred from the nearly filled $e_{g'}$ subbands to the a_{1g} band, thereby reducing orbital polarization among Co t_{2g} states. Dynamical correlations therefore stabilize the small $e_{g'}$ Fermi surface pockets, in contrast to angle-resolved photoemission data, which do not reveal these pockets.

The intercalated layer compound Na_xCoO_2 has been intensely studied during the recent years since as a function of Na doping it exhibits a variety of fascinating properties. The relevant valence bands near the Fermi level consist of Co t_{2g} states with occupancy $3d^{5+x}$. For $x \approx 0.50 - 0.75$ an unusually large thermopower is observed [1]. For $x \approx 0.3$ hydration gives rise to a superconducting transition at 4.5 K [2]. In a narrow region near $x = 0.5$ the material undergoes a metal insulator transition [3, 4]. The end-member at $x = 0$ with a single hole per Co atom is believed to be a Mott insulator. At $x = 1$, since the filled t_{2g} bands are separated by about 1.5 eV from the empty e_g bands, one finds a band insulator.

Despite considerable experimental and theoretical effort, fundamental electronic properties of Na_xCoO_2 such as the qualitative topology of the Fermi surface remain controversial and are not well understood. In the metallic phase the hexagonal Fermi surface predicted by band theory within the local density approximation (LDA) consists of a large hole pocket centered at Γ and six small hole pockets near K [5] (see Fig. 1). Because of the layered structure the t_{2g} levels split into a a_{1g} level and doubly degenerate $e_{g'}$ levels. The large Fermi surface stems mainly from the a_{1g} bands while the small hole pockets have predominantly $e_{g'}$ character. The existence of these hole pockets is thought to be crucial for the understanding of the superconducting phase [6]. On the other hand, angle resolved photoemission spectra (ARPES) for $x = 0.7$ [7] and $x = 0.6$ [8] provide evidence only for a_{1g} bands crossing the Fermi level. These data suggest that the $e_{g'}$ bands are filled due to inter-orbital charge transfer not described within the LDA. New ARPES data for $x = 0.3 \dots 0.7$ [9] and $x = 0.3$ [10] also do not show the small $e_{g'}$ hole pockets.

To address the question of possible modifications of the Fermi surface via Coulomb correlations not included in the LDA, several theoretical studies were carried out for the half-metallic, magnetic region near $x = 0.7$ [11], using the LDA+U approach [12]. For a relatively large local Coulomb energy ($U > 3$ eV), the $e_{g'}$ subbands are indeed filled. In the metallic phase, however, in particular, for Coulomb energies comparable to the single-

electron band width, it is well known that correlations have an important dynamical component not captured within the LDA+U.

The aim of this work is to elucidate the possibility of modifying the Fermi surface of $\text{Na}_{0.3}\text{CoO}_2$ via dynamical Coulomb correlations. More specifically we focus on the charge transfer between the paramagnetic t_{2g} subbands. Since only the total electron number is conserved when correlations are taken into account, the occupations of individual subbands may vary with the strength of the local intra- and inter-orbital Coulomb energies. In a single-band picture, the key effect of dynamical fluctuations is the spectral weight transfer from the quasi-particle peak near E_F to the incoherent satellites associated with the lower and upper Hubbard bands. In a multi-band ma-

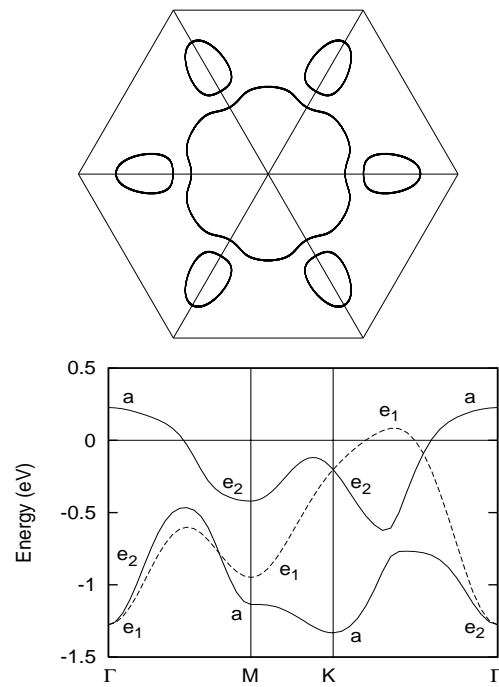


FIG. 1: Upper panel: Fermi surface of $\text{Na}_{0.3}\text{CoO}_2$. Lower panel: tight-binding fit to LDA bands; $E_F = 0$. Solid curves: even bands; dashed curve: odd band. The $e_{g'}$ states above E_F give rise to the small hole pockets of the Fermi surface.

terial, this spectral weight transfer is orbital dependent, opening the possibility of redistributing electronic charge among the valence orbitals and modifying the shape of the Fermi surface.

To investigate these multi-band correlation effects we use the dynamical mean field theory (DMFT) combined with the Quantum Monte Carlo (QMC) method [13]. The remarkable result of this work is that in the metallic domain of Na_xCoO_2 near $x = 0.3$ dynamical correlations shift charge from the $e_{g'}$ states to the a_{1g} bands, thereby stabilizing the $e_{g'}$ hole pockets and slightly reducing the a_{1g} Fermi surface. The overall topology of the Fermi surface remains the same as in the LDA.

Fig. 1 shows a tight-binding fit to the $\text{Na}_{0.3}\text{CoO}_2$ bands calculated within the LDA and using the linearized augmented plane wave (LAPW) method. We consider the paramagnetic phase observed experimentally at $x = 0.3$. Since we are interested in the qualitative issue of charge transfer between t_{2g} subbands the weak dispersion along the c -axis is neglected. The full band structure involving Co 3d and O 2p states is down-folded to a 3×3 Co t_{2g} tight-binding Hamiltonian in which on-site energies and hopping integrals represent effective energies accounting for direct Co-Co and indirect Co-O-Co interactions. Including three neighbor shells, with $dd\sigma$, $dd\pi$ and $dd\delta$ matrix elements, an excellent fit to the LAPW band structure is achieved. The details of the tight binding model and down-folding procedure will be given elsewhere [14].

Because of the planar structure of the system, it is convenient to transform the $d_{xy, xz, yz}$ orbitals into a_{1g} and $e_{g'}$ states, where $a_{1g} = (d_{xy} + d_{xz} + d_{yz})/\sqrt{3}$, $e_{g1} = (d_{xz} - d_{yz})/\sqrt{2}$, $e_{g2} = (2d_{xy} - d_{xz} - d_{yz})/\sqrt{6}$. Quantities such as the local density of states and local quasi-particle self-energy are diagonal in this representation. For instance, the a_{1g} and $e_{g'}$ density of states are $\rho_a = \rho_{ii} + 2\rho_{ij}$, $\rho_e = \rho_{ii} - \rho_{ij}$, where ρ_{ii} ($\rho_{11} = \rho_{22} = \rho_{33}$) and $\rho_{i \neq j}$ ($\rho_{12} = \rho_{13} = \rho_{23}$) are the diagonal and off-diagonal elements of the t_{2g} density of states matrix.

Fig. 2 shows the a_{1g} and $e_{g'}$ quasi-particle spectra for $\text{Na}_{0.3}\text{CoO}_2$ as calculated within the DMFT. The local Coulomb interaction defining the quantum impurity problem is characterized by intra- and inter-orbital matrix elements $U = U_{ii}$ and $U' = U_{i \neq j} = U - 2J$, where J is the Hund's rule exchange integral. The value of U for the entire t_{2g} , e_g manifold (total width about 4 eV) was estimated at 3.7 eV [15]. For the narrower t_{2g} bands a smaller value should be more appropriate to account for screening involving empty e_g states. Since accurate values of U and J are not available, DMFT calculations for several values were carried out to study their effect on the inter-orbital charge transfer. The temperatures were $T \approx 385$ and 770 K corresponding to about 30 and 60 meV thermal broadening. Up to 10^6 sweeps were done in the QMC calculations. The quasi-particle spectra are obtained via maximum entropy reconstruction [16].

The quasi-particle spectra show the characteristic band

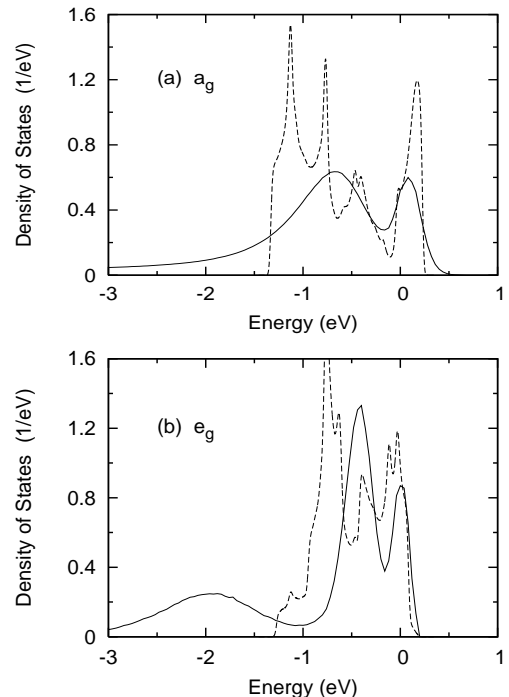


FIG. 2: Quasi-particle spectra for metallic $\text{Na}_{0.3}\text{CoO}_2$ calculated within the DMFT (solid curves) for $U = 3$ eV, $J = 0.8$ eV; $T = 770$ K, $E_F = 0$. Dashed curves: LDA local density of states. (a) a_{1g} states; (b) $e_{g'}$ states.

narrowing near E_F caused by dynamical correlations and the transfer of weight from the coherent to the incoherent spectral region. In the slightly narrower $e_{g'}$ band correlations are strong enough to give rise to a lower Hubbard band. Also noticeable is the substantial lifetime broadening of valence states due to creation of electron hole pairs. The occupations of these distributions are: $n_a = 0.853$, $n_e = 0.899$, which should be compared to the LDA values $n_a = 0.797$, $n_e = 0.927$.

To illustrate the variation of the t_{2g} subband occupations with local Coulomb and exchange energies, we show in Fig. 3(a) the trend obtained within the DMFT for $U' = U/2$, $J = U/4$ and $U' = U$, $J = 0$. In both cases charge transfer proceeds from $e_{g'}$ to a_{1g} , i.e., orbital polarization is reduced. We have evaluated the DMFT quasi-particle spectra both in the non-diagonal t_{2g} and diagonal a_{1g} , $e_{g'}$ representations. Both versions are in excellent agreement, indicating that in the present system non-diagonal coupling among t_{2g} states is fully taken into account within the a_{1g} , $e_{g'}$ representation.

The variation of the a_{1g} , $e_{g'}$ subband occupations with U derived within the DMFT differs from the one found in the LDA+U, as illustrated in Fig. 3(b). While dynamical correlations lead to reduced orbital polarization for $J = U/4$ and $J = 0$, the LDA+U treatment gives this trend only for $J = U/4$; $J = 0$ yields the opposite effect. This dependence of the orbital polarization on the ratio J/U within the LDA+U follows

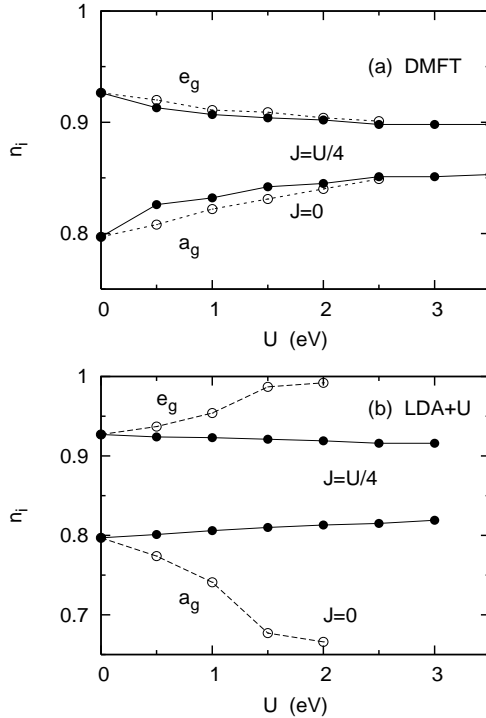


FIG. 3: Occupations of a_{1g} and $e_{g'}$ subbands of $\text{Na}_{0.3}\text{CoO}_2$ as a function of U . (a) DMFT; (b) LDA+U. Solid dots: $J = U/4$, empty dots: $J = 0$. The lines are guides for the eye.

from the Hartree Fock self-energy. For a paramagnetic t_{2g} complex with one-fold a_{1g} and two-fold $e_{g'}$ subbands, the orbital dependent potential is given by [17]: $V_{i \neq j}^{\text{LDA+U}} = \Sigma_{ij}^{\text{HF}} = \delta(U - 5J)$, with $\delta = (n_e - n_a)/3$. The diagonal term $\Sigma_{ii}^{\text{HF}} = 5\bar{n}(U - 2J)$ gives an overall energy shift, where $\bar{n} = (n_a + 2n_e)/3$. Within the a_{1g} , $e_{g'}$ basis, the self-energies are $\Sigma_a^{\text{HF}} = \Sigma_{ii}^{\text{HF}} + 2\Sigma_{ij}^{\text{HF}}$, $\Sigma_e^{\text{HF}} = \Sigma_{ii}^{\text{HF}} - \Sigma_{ij}^{\text{HF}}$. Subtracting the diagonal term the shifted band energies are: $\epsilon'_a(k) = \epsilon_a(k) + 2\delta(U - 5J)$ and $\epsilon'_e(k) = \epsilon_e(k) - \delta(U - 5J)$. Thus, for $n_e > n_a$ the a_{1g} ($e_{g'}$) energies are shifted up (down) as long as $J < U/5$. For $J > U/5$ this trend is reversed. For realistic $U = 3.0 \dots 3.5$ eV, $J \approx 0.8$ eV, the latter condition is satisfied, implying reduced orbital polarization also in the static limit.

Comparing the static self-energy with the one obtained in second-order perturbation theory [17] we find that, because of the small difference between n_a and n_e , for increasing U static correlations are rapidly dominated by dynamical correlations. Also, the more compact $e_{g'}$ density of states ensures that $\text{Re } \Sigma_e^{(2)}(\omega = 0) > \text{Re } \Sigma_a^{(2)}(\omega = 0)$ for $J = 0$ and $J = U/4$, implying diminishing orbital polarization [18]. Thus, static and dynamical correlations exhibit qualitatively different dependencies on the ratio J/U . In addition, the reduced orbital polarizations found for $J = U/4$ in the static and dynamical cases arise for different physical reasons.

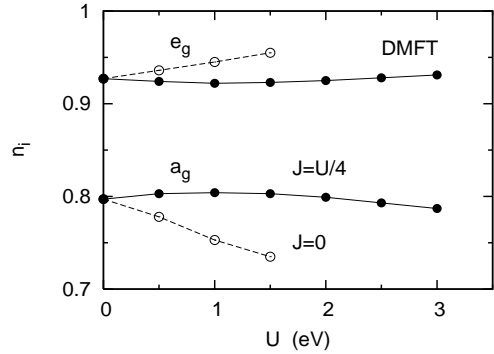


FIG. 4: Occupations of 3-band model: elliptical density of states; band fillings as in $\text{Na}_{0.3}\text{CoO}_2$; DMFT. Solid dots: $J = U/4$, empty dots: $J = 0$. The lines are guides for the eye.

The results in Fig. 3 demonstrate that in the metallic phase it is crucial to include dynamical correlations. Evidently, the new degrees of freedom generated by quasi-particle interactions, such as spectral weight transfer between low and high frequencies, relaxation shifts (band narrowing) and decay processes, which are beyond the LDA and LDA+U treatments, contribute to the charge balance between non-equivalent orbitals. It is to be expected that these dynamical correlations also depend on the single-particle bands, i.e., on the available density of occupied and unoccupied states involved in excitation processes. To illustrate this point we show in Fig. 4 the subband occupations for an analogous 3-band model with elliptical density of states and total occupancy 5.3. Adjusting the chemical shift to simulate the a_{1g} , $e_{g'}$ occupations of $\text{Na}_{0.3}\text{CoO}_2$ we find increasing orbital polarization for $J = 0$ but weakly varying n_i for $J = U/4$ [19]. Clearly, the inter-orbital charge transfer depends on the combination of single- and many-particle interactions.

The correlation induced band narrowing seen in Fig. 2 is consistent with infrared optical data [4] which show transitions within the t_{2g} manifold at lower energies than predicted by the LDA [15]. Substantial band narrowing is also observed in all ARPES measurements [7, 8, 9, 10]. On the other hand, the present results are in conflict with the ARPES data as far as the filling of the $e_{g'}$ bands is concerned. So far, we have no explanation for this qualitative discrepancy between our state-of-the-art DMFT results and the ARPES data. The interpretation of photoemission spectra can be complicated due to surface induced single-particle and correlation features [20]. Moreover, matrix element effects could play a role. For instance, along ΓK (chosen as x axis) the a_{1g} and $e_{g'}$ bands are even with respect to $\pm(y, z)$ where z defines the surface normal (see Fig. 1). In contrast, e_{g1} is odd. These states therefore couple differently to the incident photon field. To identify the orbital character of the t_{2g} bands near E_F the use of various polarizations is recommended.

It is interesting to compare the influence of dynamical correlations on the subband occupations of $\text{Na}_{0.3}\text{CoO}_2$ to those found in other multi-band materials. The t_{2g} valence bands of the layer perovskite Sr_2RuO_4 also have a_{1g} , $e_{g'}$ symmetry, but are 2/3 filled. Because of the smaller width of the $e_{g'}$ bands DMFT predicts a charge transfer to the a_{1g} band [17], shifting the a_{1g} van Hove singularity closer to E_F than in the LDA [21]. The basic shape of the Fermi surface is preserved. The transfer from $e_{g'}$ to a_{1g} agrees with the one found here for $\text{Na}_{0.3}\text{CoO}_2$. A similar inter-orbital charge transfer was recently obtained in DMFT calculations for BaVS_3 [22]. In the orthorhombic phase this $3d^1$ material exhibits a wide a_{1g} band and weakly occupied, narrow $e_{g'}$ bands. Dynamical correlations were found to cause a transfer of electrons from a_{1g} to $e_{g'}$ states, thereby reducing orbital polarization. As in the present system, the same trend was obtained for small and large Hund's rule exchange terms ($J = U/7$, $U/4$). On the other hand, as recently shown by Pavarini *et al.* [23] for several $3d^1$ perovskites, non-diagonal t_{2g} coupling caused by octahedral distortions decreases orbital fluctuations and enhances insulating behavior. Also, Manini *et al.* [24] studied the Mott transition in a model consisting of two equal subbands with unit total occupancy. With increasing chemical shift, causing more diverse band fillings, the tendency towards a Mott insulator was found to be enhanced. Since in their case $J = 0$, these results are consistent with the enhanced orbital polarization shown in Fig. 4 for $J = 0$. These various trends underscore the subtle nature of correlations in multi-band systems, and their remarkable sensitivity to various system parameters, in particular, the shape of the density of states and the size of J/U .

In summary, we have explored the modification of the Fermi surface of $\text{Na}_{0.3}\text{CoO}_2$ as a result of dynamical correlations. The main effect of these fluctuations is the spectral weight transfer from the quasi-particle peak near E_F to the incoherent part of the spectrum. In a multi-band material, these dynamical processes are orbital dependent. In particular, since they depend on orbital occupations, they can give rise to charge transfer between subbands induced via hybridization and inter-band Coulomb interactions. The highlight of the LDA band structure of $\text{Na}_{0.3}\text{CoO}_2$ is the distinctly different filling of the t_{2g} bands, with the nearly full $e_{g'}$ subbands yielding characteristic hole pockets of the Fermi surface. Accounting for correlations within the DMFT we have shown that electronic charge is shifted from the $e_{g'}$ subbands to the a_{1g} band, thus slightly enlarging the small $e_{g'}$ hole pockets and reducing the main a_{1g} pocket centered at Γ . Further studies are needed to reconcile these theoretical findings with the photoemission data.

We like to thank O. Gunnarsson and I. I. Mazin for useful comments.

Email address: ishida@chs.nihon-u.ac.jp; johannes@dave.nrl.navy.mil; a.liebsch@fz-juelich.de

- [1] I. Terasaki, Y. Sasago and K. Uchinokura, Phys. Rev. B **56**, 12685 (1997).
- [2] K. Takada *et al.*, Nature **422**, 53 (2003); R. E. Schaak *et al.*, Nature **424**, 527 (2003).
- [3] M. L. Foo *et al.*, Phys. Rev. Lett. **92**, 247001 (2004).
- [4] N. L. Wang *et al.*, cond-mat/0405218.
- [5] D. J. Singh, Phys. Rev. B **61**, 13397 (2000).
- [6] K. Kuroki, Y. Tanaka and R. Arita, Phys. Rev. Lett. **93**, 077001 (2004); M. D. Johannes, I. I. Mazin, D. J. Singh and D. A. Papaconstantopoulos, Phys. Rev. Lett. **93**, 097005 (2004); M. Mochizuki, Y. Yanase and M. Ogata, cond-mat/0407094.
- [7] M. Z. Hasan *et al.*, Phys. Rev. Lett. **92**, 246402 (2004).
- [8] H.-B. Yang *et al.*, Phys. Rev. Lett. **92**, 246403 (2004).
- [9] H.-B. Yang *et al.*, cond-mat/0501403.
- [10] M. Z. Hasan *et al.*, cond-mat/0501530.
- [11] L.-J. Zou, J.-L. Wang and Z. Zeng, Phys. Rev. B **69**, 132505 (2004); K.-W. Lee, J. Kunes and W. Picket, Phys. Rev. B **70**, 045104 (2004); P. Zhang *et al.*, Phys. Rev. B **70**, 085108 (2004); Phys. Rev. Lett. **93**, 236402 (2004); K.-W. Lee, J. Kunes, P. Novak and W. Picket, cond-mat/0408411.
- [12] A. I. Liechtenstein, V. I. Anisimov, and J. Zaanen, Phys. Rev. B **52**, R5467 (1995).
- [13] For a review, see: A. Georges, G. Kotliar, W. Krauth and M. J. Rozenberg, Rev. Mod. Phys. **68**, 13 (1996).
- [14] O.K. Andersen, I. I. Mazin, O. Jepsen, M. Johannes, and A. Yamasaki, to be published.
- [15] M. D. Johannes, I. I. Mazin, and D. J. Singh, cond-mat/0408696.
- [16] M. Jarrell and J. E. Gubernatis, Phys. Rep. **269**, 133 (1996).
- [17] A. Liebsch and A. I. Lichtenstein, Phys. Rev. Lett. **84**, 1591 (2000).
- [18] The same trend is found in fluctuation exchange calculations; M. Mochizuki, Y. Yanase and M. Ogata, cond-mat/0503252. The self-energy in this approach is momentum dependent and includes pair exchange terms. Both features are absent in the QMC/DMFT. On the other hand, going beyond LDA+U by using a Gutzwiller ansatz, Zhou *et al.*, cond-mat/0503346, find enhanced orbital polarization in the strong-coupling $U \rightarrow \infty$ limit. It would be interesting to extend these calculations to realistic values of U , J .
- [19] The trend for $J = U/4$ suggests enhanced orbital polarization in the limit of large U .
- [20] K. Maiti *et al.*, Europhys. Lett. **55**, 246 (2001); A. Sekiyama *et al.*, Phys. Rev. Lett. **93**, 156402 (2001); A. Liebsch, Phys. Rev. Lett. **90**, 96401 (2003); Eur. Phys. J. **32**, 477 (2003).
- [21] T. Oguchi, Phys. Rev. B **51**, 1385 (1995); I. I. Mazin and D. J. Singh, Phys. Rev. Lett. **79**, 733 (1997).
- [22] F. Lechermann, S. Biermann, and A. Georges, cond-mat/0409463.
- [23] E. Pavarini, S. Biermann, A. Poteryaev, A. I. Lichtenstein, A. Georges, and O. K. Andersen, Phys. Rev. Lett. **92**, 176403 (2004).
- [24] N. Manini, G. Santoro, A. Dal Costa and E. Tosatti, Phys. Rev. B **66**, 115107 (2002).